# Extended corresponding states for pure polar and non-polar fluids: an improved method for component shape factor prediction

Isabel M. Marrucho [a], James F. Ely [b,*]

[a] *Instituto Superior Técnico, Universidade Técnica de Lisboa, Lisbon, Portugal*
[b] *Chemical Engineering and Petroleum Refining Department, Colorado School of Mines, Golden, CO 80401, USA*

## Abstract

In the past, the extended corresponding states approach to fluid property prediction has been restricted to non-polar fluids (e.g., hydrocarbons and some common non-polar inorganics) due to the lack of an accurate way to predict the required shape factors. In this work, a new predictive method to obtain shape factors for the extended corresponding states theory (ECST) has been developed which is applicable to both polar and non-polar fluids. The details of this revised extended corresponding states model are presented. The resulting model has been applied with success to a wide variety of pure fluids including alcohols, amines, ethers and substituted aromatics. Detailed extended corresponding states shape factor results are presented here for hydrocarbons, alkenes, non-polar inorganics, polar inorganics and refrigerants. © 1998 Elsevier Science B.V. All rights reserved.

*Keywords:* Extended corresponding states theory; Phase equilibria; Polar fluids; *PVT*; Shape factors

## 1. Introduction

Polarity and association profoundly affect the phase behavior and the single phase properties of fluids. Most approaches used to represent the thermodynamic properties of polar fluids have been based upon empirical modifications of engineering equations of state. Usually these modifications involve the addition of one or more parameters which account for the polar effects. More sophisticated models are based on perturbation theory and include the perturbed-hard-chain theory family (PCT), with different modifications according to the properties of interest, the chain of rotators

---

* Corresponding author. Tel.: +1-3032733885; fax: +1-3032733730; e-mail: jely@mines.edu

(COR), the Boublick–Alder–Chen–Kreglewski (BACK) equation of state and the statistical association fluid theory (SAFT). A detailed review of these models as well as others is given in Ref. [1].

One the of more accurate approaches to predicting properties of non-polar fluids, the extended corresponding states theory (ECST), has not found much success for polar fluids. This has been due to the inaccurate prediction of the shape factors required in the ECST model and the simple mixing rules typically used with this approach. The potential advantages of this model are the incorporation of high accuracy reference fluid equations of state and the well-defined theoretical approximations which underlay its application. The revised ECST model reported here presents a new way of predicting and/or correlating component shape factors. It has been applied with success to a wide variety of pure fluids including alcohols, amines, ethers and substituted aromatics, both for single phase and equilibrium properties.

## 2. Revised ECST shape factors for pure fluids

In the late 1970s and early 1980s, high accuracy equations of state based on wide-range experimental data for homologous series became available, which made possible the exact (although numerical) calculation of shape factors. Given these high accuracy equations of state, shape factors can be found from the simultaneous solution of the equations,

$$a_j^r(V_j, T_j) = a_0^r(V_0, T_0) = a_0^r(V_j/h_j, T_j/f_j) \tag{1}$$

and

$$z_j^r(V_j, T_j) = z_0^r(V_0, T_0) = z_0^r(V_j/h_j, T_j/f_j) \tag{2}$$

where the scaling factors $f_j$ and $h_j$ are defined below and a notation has been introduced in which a dimensionless residual property is denoted by a lower case letter with a superscript 'r'. For example, in Eq. (1) above $a_0^r \equiv [A_0(V_0, T_0) - A_0 * (V_0, T_0)]/RT$ where '∗' denotes an ideal gas value. The mathematical details of the implementation of the ECST are given in the literature [2].

For the great majority of fluids, the high accuracy equations of state required to solve Eqs. (1) and (2) are not available. Thus, the application the ECST for those fluids requires the prediction of the shape factors. So far, the exact shape factors have been found to be temperature and density dependent. However, it is possible to calculate shape factors which are density independent and are a good representation of the exact ones in certain parts of the phase diagram.

### 2.1. Subcritical shape factors

A good example of density independent shape factors are those obtained from the mapping of the saturation boundaries of the reference fluid '0' and the target fluid '$j$' by simultaneous solution of the following equations [3]:

$$P_j^{sat}(T_j) = p_0^{sat}(T_j/f_j)h_j/f_j \tag{3}$$

$$\rho_j^{sat,1}(T_j) = \rho_0^{sat,1}(T_j/f_j)/h_j \tag{4}$$

where $P^{sat}$ and $\rho^{sat}$ represent the saturated pressure and density, $T$ denotes the temperature and $f_j$ and $h_j$ are the equivalent substance reducing ratios, which are defined as functions of the shape factors, $\theta(V,T)$ and $\phi(V,T)$,

$$h_j = \left(V_j^c/V_0^c\right)\phi(V,T) \text{ and } f_j = \left(T_j^c/T_0^c\right)\theta(V,T) \tag{5}$$

The exponent 'c' denotes the critical property. Analysis of the exact shape factors in the subcritical region shows weak density dependence, thus allowing, to a very good approximation, the use of the saturated shape factors in this region. As summarized in Ref. [4], shape factors determined from Eqs. (1)–(5) have been fitted to simple functions of reduced temperature such as

$$\theta = 1 + (\omega - \omega_0)\left[a_1 + a_2 \ln(T*)\right] \tag{6}$$

and

$$\Phi = \left(\frac{Z^c}{Z_0^c}\right)\phi = 1 - (\omega - \omega_0)\left[b_1 + b_2 \ln(T*)\right] \tag{7}$$

and then used to make ECST predictions over the entire thermodynamic surface. In this work we have developed improved functional forms to represent the shape factors and better methods to predict the parameters used in those functional forms.

In order to calculate the shape factors along the saturation boundary, analytical expressions for the saturated pressure and liquid density must be known. The simplest equation for correlation of the vapor pressure with a sound physical basis is the Frost–Kalkwarf equation [5], which in its reduced form can be written as

$$\ln p^{*,sat} = B * \left(\frac{1}{T*} - 1\right) + C * \ln T * + D * \left(\frac{P^{*,sat}}{T*^2} - 1\right) \tag{8}$$

where the superscript '$*$' denotes a reduced value of the related quantities. $D*$ is a universal constant $27/64$ and $B*$ and $C*$ depend upon the material under consideration. For the liquid density, the Rackett equation gives a compact yet amazingly accurate means to estimate saturated liquid volumes. In its original form it can be expressed as [6]:

$$V^{sat} = V^c\left(Z^c\right)^{(1-T*)^{2/7}} \tag{9}$$

Using Eqs. (3)–(5) and (8), the $\theta$ shape factor can be written as

$$\theta = \frac{1 - C_0 * + \ln\Phi - \Delta B * + \Delta C * \ln T_j * + B_j * /T_j * + D * P_j^{sat,*}(1 - \theta\Phi)/T_j *^2}{1 - C_0 * + B_0 * /T_j *} \tag{10}$$

In deriving Eq. (10), we have assumed that $\theta$ is close to one and therefore $\ln\theta \cong \theta - 1$ and have defined $\Phi = \phi(Z_j^c/Z_0^c)$, $\Delta B * = B_j * - B_0 *$ and $\Delta C * = C_j * - C_0 *$. Analysis of exact shape factor data along the saturation boundary shows that the term that multiplies $D*$ is very small, contributing

at most 0.005 to the shape factor in a small region near the critical point. Away from the critical point it typically contributes less than 0.00001. Thus, the term was neglected. Since there are two unknowns remaining, $\theta$ and $\Phi$, another equation is needed. At saturation, $h_j$ is given by

$$h_j = \frac{V_j^c}{V_0^c} \phi = \frac{V_j^{\text{sat}}(T_j*)}{V_0^{\text{sat}}(T_j*/\theta)} \tag{11}$$

If the Rackett equation [6] is used to calculate the saturated liquid volumes, the expression for $\phi$ becomes

$$\phi = \frac{\left(Z_j^c\right)^{(1-T_j*)^{2/7}}}{\left(Z_0^c\right)^{(1-T_j*/\theta)^{2/7}}} . \tag{12}$$

As a first order approximation for $\phi$ that is independent of $\theta$, we assume that $\theta \cong 1$ and that, $\Phi \approx \phi$. The exponent of two is based on empirical observation and we note that more complicated approximations are possible. The net result of these manipulations is our final expression for the $\theta$ shape factor

$$\theta = \frac{1 - C_0* + 2\left(1 - T_j*\right)^{2/7}\ln\left(Z_j^c/Z_0^c\right) - \Delta B* + \Delta C*\ln T_j* + B_j*/T_j*}{1 - C_0* + B_0*/T_j*} \tag{13}$$

Note that as a consequence of our approximation concerning $\Phi$, $\theta$ approaches unity at the critical point. It is also important to note a very important feature of the shape factor formulas given in Eqs. (12) and (13). In particular, this formulation is easily transferable between reference fluids since the reference fluid parameters appear explicitly in the shape factors. This should be compared to the formulation given in Eqs. (6) and (7) which is reference fluid specific and can only be used with other reference fluids through cumbersome transformation formulas [4].

Given this new formulation, it is possible to correlate the $\theta$ and $\phi$ shape factors by fitting $B*$ and $C*$ in Eq. (13) and $Z_j^c$ and the exponent $\varepsilon (= 2/7$ in the original Eq. (12)) in the Rackett equation to saturation data. Fig. 1 illustrates the results that can be obtained from these equations for *n*-pentane as compared to the exact values for the shape factors obtained from Eqs. (1) and (2). The agreement, even in the vicinity of the critical point, is excellent.

Since the goal of corresponding states theory is to predict fluid properties given a minimum of information, typically the critical point parameters and acentric factor, a relationship between $B*$ and $C*$ and the parameters available in a corresponding states calculation is required. By plotting experimental data for non-polar and non-hydrogen bonding polar substances, Reynes and Thodos [7], found that $C* = 8/3 + 9B*/5 \ln 10$. Thus, it only remains to determine one parameter, $B*$, per fluid. Using the observed relationship between $B*$ and $C*$ and Eq. (8) to calculate the acentric factor, it is easy to show that $B*$ can be written in terms of $\omega$ as

$$B* = b_1 + b_2\omega + b_3 10^{-\omega} \tag{14}$$

where for the relationship between $B*$ and $C*$ given above, $b_1 = -6.207612$, $b_2 = -15.37641$ and $b_3 = -0.574946$. Thus, in the subcritical region, the relationships developed here can be used in either a correlative or predictive mode, given the information available.
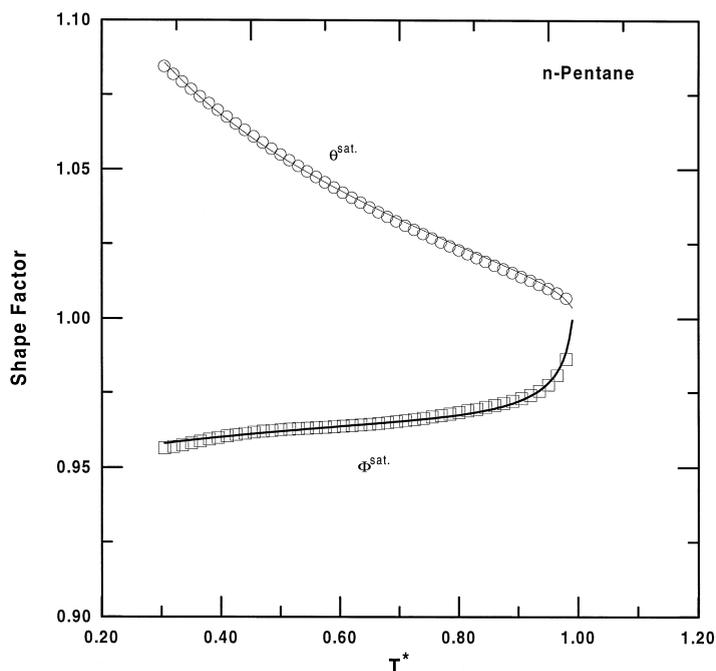
Fig. 1. Comparison of correlated subcritical *n*-pentane shape factors obtained with Eqs. (12) and (13) to exact values calculated with Eqs. (1) and (2).

## 2.2. Supercritical shape factors

At supercritical conditions there is no accepted, accurate way to estimate the shape factors. Several unique lines in this region have been analyzed in this study, including, the critical isochore and the zeno (unit compressibility factor) line [8]. Fig. 2 illustrates the exact shape factors found along these lines and the saturation boundary for methane. In examining Fig. 2, we conclude that in the single-phase region where the lines do not coincide, it is not possible to characterize the behavior of a fluid without the introduction of density dependence in the shape factors. The observed density dependence in the shape factors in this region can in part be due to uncertainties in the equations of state (according to the techniques used in their construction) and in the experimental data upon which they depend. We contend, however, that this apparent density dependence is primarily due to the fact that the two-parameter corresponding states principle requires that the critical compressibility factors of the target and reference fluids be identical at the critical point—something that is not generally observed in nature. Thus, we see a strong 'hook' in the subcritical shape factors at the critical point and a near-critical region where two temperature dependent only paths give different values for $\theta$ and $\Phi$.

From the two-parameter corresponding states relation for the pressure at the critical point of the target fluid we find that

$$\Phi^c = \left(\frac{Z^c}{Z_0^c}\right)\phi^c = p_0 * \left(\frac{1}{\theta^c}, \frac{1}{\phi^c}\right)\theta^c$$
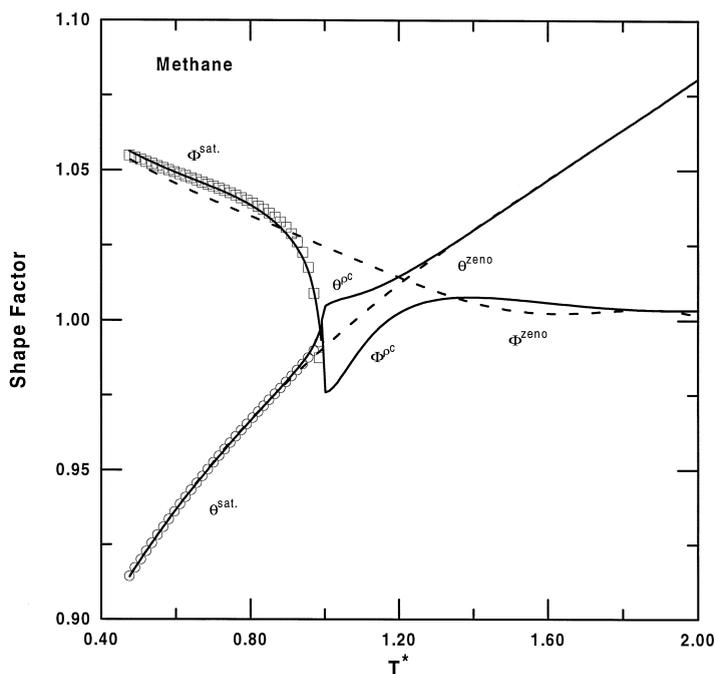
Fig. 2. Illustration of the lack of correspondence along the critical isochore and zeno line for methane. The dashed curves are the shape factors on the zeno line while the solid lines show values along the critical isochore.

Our construction of $\theta$ as given in Eq. (13) requires that $\theta^c$ be unity which places the reference fluid on its critical isotherm, where for a fairly large region around the critical point $P_0* \cong 1$. Thus, the limiting subcritical value of $\phi$ is $Z_0^c/Z^c$ and we have chosen to set $\phi$ equal to this constant value in the supercritical region. Note that there is large precedent for this approximation, since this is the

Table 1
Comparison of exact and correlated subcritical shape factors

| Fluid type | Np | $\theta$ Shape factor | | | | | | $\phi$ Shape factor | | | | | |
| | | Eq. (13) | | | Eq. (6) | | | Eq. (12) | | | Eq. (7) | | |
| | | AAD (%) | RMS (%) | BIAS (%) | AAD (%) | RMS (%) | BIAS (%) | AAD (%) | RMS (%) | BIAS (%) | AAD (%) | RMS (%) | BIAS (%) |
|---|---|---|---|---|---|---|---|---|---|---|---|---|---|
| Hydrocarbons[a] | 1258 | 0.08 | 0.09 | −0.05 | 0.08 | 0.10 | 0.00 | 0.16 | 0.19 | −0.04 | 0.15 | 0.21 | 0.00 |
| Alkenes[b] | 258 | 0.09 | 0.11 | −0.06 | 0.07 | 0.08 | 0.00 | 0.58 | 0.66 | 0.22 | 0.11 | 0.16 | 0.00 |
| Non-polar inorganics[c] | 442 | 0.07 | 0.11 | −0.04 | 0.12 | 0.16 | 0.00 | 0.36 | 0.48 | 0.08 | 0.41 | 0.52 | 0.00 |
| Polar inorganics[d] | 398 | 0.09 | 0.12 | −0.05 | 0.21 | 0.26 | 0.00 | 1.09 | 1.33 | −0.20 | 0.94 | 1.16 | 0.02 |
| Refrigerants[e] | 1135 | 0.06 | 0.07 | −0.03 | 0.09 | 0.12 | 0.00 | 0.15 | 0.18 | 0.00 | 0.43 | 0.55 | 0.01 |
| Overall | 3491 | 0.07 | 0.09 | −0.05 | 0.10 | 0.13 | 0.00 | 0.32 | 0.39 | −0.01 | 0.36 | 0.46 | 0.00 |

[a]Hydrocarbons: methane, ethane, *n*-butane, *i*-butane, *n*-pentane, *i*-pentane, *n*-hexane, *i*-hexane, *n*-heptane, cyclohexane.
[b]Alkenes: ethylene, propylene.
[c]Non-polar Inorganics: oxygen, nitrogen, carbon dioxide, argon, neon.
[d]Polar Inorganics: ammonia, water, hydrogen sulfide, carbon monoxide.
[e]Refrigerants: R11, R12, R22, R32, R123, R124, R125, R134a, R143a, R152a.

result obtained from simple (two-parameter) engineering equations of state where the volume parameter is temperature independent [9] and all fluids have the same critical compressibility factor. As for $\theta$, we assume that the critical isochore of the target fluid is linear and map that isochore onto a nearby (assumed linear) isochore of the reference fluid via the following relationship,

$$f = \frac{T_j^c}{T_0^c}\, \theta = \frac{h_0\left(p_j^c - T_j^c \gamma_j^c\right) + \left(h_0 \gamma_j^c - \gamma_0^\sigma\right)T_j}{p_0^\sigma - \gamma_0^\sigma T_0^\sigma} \tag{15}$$

where the superscript '$\sigma$' indicates the isochore which intersects the reference fluid saturation boundary at $\rho_0^\sigma = \rho h_0$, $h_0 = Z_0^c \rho_0^c / Z_j^c \rho_j^c$ and $\gamma \equiv (\partial P/\partial T)\rho$. $\gamma^c$ for the target fluid may be obtained from the Frost–Kalkwarf equation where ($\alpha = 1$) as

$$\gamma_j^c = \alpha p_j^c \left(C_j^* - B_j^* - 2D^*\right)\big/(1 - D*)T_j^c . \tag{16}$$

Our studies have shown that with $\alpha = 1$, Eq. (16) tends to underestimate the slope of the critical isochore by about 2%. Thus we have empirically set $\alpha = 1.02$.

## 3. Results

In Section 2, a new technique for correlating and predicting shape factors, which allows a more accurate description of the phase diagram, especially in the subcritical region, was developed. This new method has been applied to 325 pure fluids from several families already mentioned. In order to compare with previous implementations of ECST, we are only reporting results for 31 fluids for which we have high accuracy, wide range equations of state. Table 1 compares the results obtained by correlating the subcritical shape factors with the new and old functional forms for typical fluids investigated in this study. Table 2 presents comparable results obtained by using the two models in a predictive mode where only the critical point and acentric factor are given as input. Table 3 presents the results of predicting the supercritical shape factors along the critical isochore using the new and old procedures. The improved performance of the new predictive methods, especially in the subcritical region, is obvious. Also, this new method allows a more accurate correlation and

Table 2
Comparison of exact and predicted subcritical shape factors

| Fluid type[a] | Np | $\theta$ Shape factor | | | | | | | | | | | | $\phi$ Shape factor | | | | | | | | | | | |
|---|---|---|---|---|---|---|---|---|---|---|---|---|---|---|---|---|---|---|---|---|---|---|---|---|---|---|
| | | Eq. (13) | | | Eq. (6) | | | Eq. (12) | | | Eq. (7) | | |
| | | AAD (%) | RMS (%) | BIAS (%) | AAD (%) | RMS (%) | BIAS (%) | AAD (%) | RMS (%) | BIAS (%) | AAD (%) | RMS (%) | BIAS (%) |
| Hydrocarbons | 1258 | 0.17 | 0.15 | 0.05 | 0.22 | 0.25 | 0.02 | 0.25 | 0.21 | 0.04 | 0.53 | 0.40 | −0.11 |
| Alkenes | 258 | 0.34 | 0.09 | −0.31 | 0.21 | 0.25 | −0.01 | 0.57 | 0.72 | −0.06 | 0.70 | 0.34 | −0.51 |
| Non-polar inorganics | 442 | 0.16 | 0.14 | −0.10 | 0.43 | 0.23 | 0.36 | 0.43 | 0.54 | 0.07 | 1.77 | 0.70 | −1.73 |
| Polar inorganics | 398 | 0.54 | 0.46 | 0.02 | 1.23 | 0.74 | −0.80 | 1.14 | 1.38 | −0.14 | 9.15 | 1.70 | 7.77 |
| Refrigerants | 1135 | 0.20 | 0.19 | 0.11 | 0.49 | 0.34 | 0.36 | 0.19 | 0.17 | 0.10 | 3.61 | 0.90 | 2.93 |
| Overall | 3491 | 0.23 | 0.19 | 0.02 | 0.45 | 0.33 | 0.16 | 0.38 | 0.41 | 0.04 | 2.69 | 0.75 | 1.54 |

[a]Fluid type groupings are defined in Table 1.

Table 3
Comparison of exact and predicted supercritical shape factors

| Fluid type[a] | Np | $\theta$ Shape factor | | | | | | $\phi$ Shape factor | | | | | |
| | | Eq. (15) | | | Eq. (6) | | | $\phi = Z_0^c / Z^c$ | | | Eq. (7) | | |
| | | AAD (%) | RMS (%) | BIAS (%) | AAD (%) | RMS (%) | BIAS (%) | AAD (%) | RMS (%) | BIAS (%) | AAD (%) | RMS (%) | BIAS (%) |
|---|---|---|---|---|---|---|---|---|---|---|---|---|---|
| Hydrocarbons | 510 | 0.96 | 0.77 | 0.59 | 0.72 | 0.62 | 0.32 | 3.06 | 1.85 | −2.69 | 3.61 | 1.94 | −2.95 |
| Alkenes | 102 | 0.39 | 0.38 | 0.17 | 0.55 | 0.59 | −0.20 | 1.65 | 1.82 | −0.30 | 2.26 | 2.41 | 1.13 |
| Non-polar inorganics | 255 | 0.69 | 0.49 | −0.41 | 1.91 | 1.24 | −1.69 | 7.27 | 5.25 | 6.72 | 7.13 | 5.49 | 6.36 |
| Polar inorganics | 204 | 0.56 | 0.40 | 0.40 | 1.12 | 0.75 | −0.79 | 3.37 | 2.79 | 2.75 | 3.10 | 3.06 | 2.01 |
| Refrigerants | 255 | 0.28 | 0.30 | 0.11 | 1.16 | 0.87 | −0.42 | 3.73 | 3.28 | 0.29 | 4.07 | 3.50 | −0.84 |
| Overall | 1326 | 0.67 | 0.54 | 0.24 | 1.08 | 0.81 | −0.42 | 3.94 | 2.92 | 0.71 | 4.19 | 3.13 | 0.32 |

[a]Fluid type groupings are defined in Table 1.

prediction of the shape factors in the near-critical region than was previously possible. Since the accuracy of the calculated thermodynamic properties is a reflection of the accuracy of the shape factors themselves, the description of the fluids through this new formulation will be significantly improved compared to the previous ECST formulation.

## 4. Summary and conclusions

In this work we have developed new methods for correlating and predicting the component shape factors for the extended corresponding states approach to fluid properties. Unlike previous methods, these methods are transferable from one reference fluid to another, are not limited to non-polar substances and, therefore, offer a means of making more accurate predictions for polar fluids. Future work will include the incorporation of more sophisticated mixing rules in the revised extended corresponding states model so that more accurate predictions may be made for polar–polar and polar–non-polar mixtures.

## Acknowledgements

## References

[1] I.M. Marrucho-Ferreira, Extended Corresponding States Theory: Application for Polar Compounds and Their Mixtures, PhD Thesis, University of Lisbon, 1997.
[2] J.F. Ely, Adv. Cryo. Eng. 35 (1990) 1520.
[3] A.S. Cullick, J.F. Ely, J. Chem. Eng. Data 27 (1982) 276.

[4] J.F. Ely, I.M.F. Marrucho, The corresponding states principle, in: J.V. Sengers (Ed.), Equations of State for Fluids and Fluid Mixtures, Blackwell, Oxford, 1997.

[5] A. Frost, D.R. Kalkwarf, J. Chem. Phys. 21 (3) (1953) 264.

[6] H.G. Rackett, J. Chem. Eng. Data 15 (1970) 514.

[7] E.G. Reynes, G. Thodos, Ind. Eng. Chem. Fundam. 1 (2) (1962) 127.

[8] J. Xu, D.R. Herschbach, J. Phys. Chem. 96 (1992) 2307.

[9] J. Mollerup, Fluid Phase Equilib. 4 (1980) 11.